JOC Article
pubs.acs.org/joc

# Structure Elucidation of Dimethylformamide-Solvated Alkylzinc Cations in the Gas Phase

Frank Dreiocker,[†] Jos Oomens,[‡,§] Anthony J. H. M. Meijer,[⊥] Barry T. Pickup,[⊥] Richard F. W. Jackson,*[,⊥] and Mathias Schäfer*[,†]

[†]*Department of Chemistry, Institute for Organic Chemistry, University of Cologne, Greinstrasse 4, 50939 Köln, Germany,* [‡]*FOM Institute for Plasma Physics Rijnhuizen, Edisonbaan 14, Nieuwegein 3439 MN, The Netherlands,* [§]*University of Amsterdam, Nieuwe Achtergracht 166, 1018WV Amsterdam, The Netherlands, and* [⊥]*Department of Chemistry, The University of Sheffield, Dainton Building, Sheffield, S3 7HF, United Kingdom*

*mathias.schaefer@uni-koeln.de; r.f.w.jackson@sheffield.ac.uk*

*Received November 23, 2009*

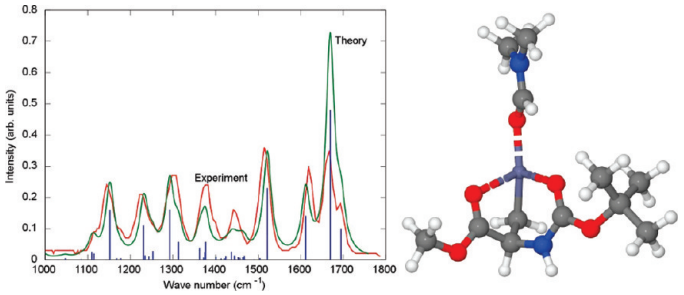


Organozinc iodides, useful for the synthesis of nonproteinogenic amino acids, are investigated in the gas phase by a combination of electrospray (ESI)-MS/MS, accurate ion mass measurements, and infrared multiphoton dissociation (IRMPD) spectroscopy employing a free electron laser. ESI allowed the full characterization of a set of dimethylformamide (DMF)-solvated alkylzinc cations formed by formal loss of $I^-$ in the gas phase. Gas phase ion structures of the organozinc cations were identified and optimized by computations at the B3LYP/6-311G** level of theory. The calculations indicate that the zinc cation in gas phase alkylzinc-DMF species preferentially adopts a tetrahedral coordination sphere with four ligands, namely the alkyl group, any internal coordinating group, and DMF (the number of which depends on the number of internal coordinating groups present). Besides the sequential loss of coordinated DMF, collision-induced dissociation (CID) patterns demonstrate that the zinc-DMF interaction in tetrahedral four-coordinate mono-DMF-zinc complex ions can be even stronger than covalent bonds. The IRMPD spectra of the alkylzinc-DMF species examined show a rich pattern of indicative bands in the range of 1000−1800 $cm^{-1}$. All major features of the recorded IRMPD spectra are consistent with the computed IR spectra of the respective gas phase ion structures predicted by theory, allowing identification and assignment.

## Introduction

The functional group compatibility of organozinc reagents ensures that they are among the most flexible sources of carbon nucleophiles available.[1,2] Functionalized alkylzinc iodides are compatible with acidic protons,[3] including phenolic protons[4] and trifluoroacetamides,[5] and even water,[6,7] attesting to the lack of basicity of these reagents. The reasons

*To whom correspondence should be addressed. Phone: ++49 221 470 3086. Fax: ++49 221 470 3064.

(1) Knochel, P.; Singer, R. D. *Chem. Rev.* **1993**, *93*, 2117–2188.
(2) Knochel, P.; Jones P. In *Organozinc Reagents: A Practical Approach*; Oxford University Press: Oxford, UK, 1999.
(3) Knoess, H. P.; Furlong, M. T.; Rozema, M. J.; Knochel, P. *J. Org. Chem.* **1991**, *56*, 5974–5978.
(4) Jackson, R. F. W.; Rilatt, I.; Murray, P. J. *Org. Biomol. Chem.* **2004**, *2*, 110–113.
(5) Rilatt, I.; Jackson, R. F. W. *J. Org. Chem.* **2008**, *73*, 8694–8704.

DOI: 10.1021/jo902492z Published on Web 01/20/2010

for this behavior, which is somewhat counterintuitive, are at present not well understood.

Much of the recent progress in the applications of functionalized alkylzinc iodides has relied on the empirical observation that dipolar aprotic solvents are beneficial both for the preparation and solution stability of the reagents.[8] For example, dimethylformamide (DMF) has been employed as solvent for reactions of amino acid-derived alkylzinc reagents.[9] In a recent paper, we have reported the detection of a large set of solvated alkylzinc cations derived from solutions of alkylzinc iodides in absolute DMF using electrospray ionization mass spectrometry (ESI-MS) in positive ion mode.[10] The high abundances of alkylzinc complex cations observed in these experiments suggest easy and efficient ionization of the zinc−iodine bond under these conditions. Moreover, high-level DFT calculations suggest that coordination of three DMF molecules to alkylzinc iodides can induce tight ion pair formation, which might explain the ease of formation of solvated cations in the ESI experiment.[10] Furthermore, ion structures of the alkylzinc complex ions identified by theory established that DMF coordinates strongly to zinc, influencing the intramolecular coordination by the carbonyl oxygen atoms of both the carbamate protecting group and the ester of the derivatized amino acid precursor molecules (see Scheme 1).[10] Finally, the ease of ionization of the zinc−iodine bond provides a credible explanation for the low reactivity of alkylzinc iodides both as nucleophiles and as bases, and thus the broad functional group tolerance of alkylzinc iodides,[1,2,9] as well as the need for intramolecular coordination of zinc by the carbamate group in the syn $\beta$-elimination of $\beta$-Boc-amino alkylzinc iodides.[11]

To better understand the structure of DMF-solvated alkylzinc cations and the nature and relative strength of the interactions with DMF solvent molecules, we have undertaken an extended gas phase study using a combination of ESI[12−14] and collision activation dissociation (CID) tandem mass spectrometry (MS/MS).[15] ESI has frequently proven to be an efficient method for transferring even labile metal-coordinated complexes from solution to the gas phase.[16−20] In particular, following our initial work, closely related studies on the nature of solvated alkylzinc cations

**SCHEME 1. Precursor Alkylzinc Iodides 1−5 and Gross Structures of the Solvated Cations Formed by ESI-MS**

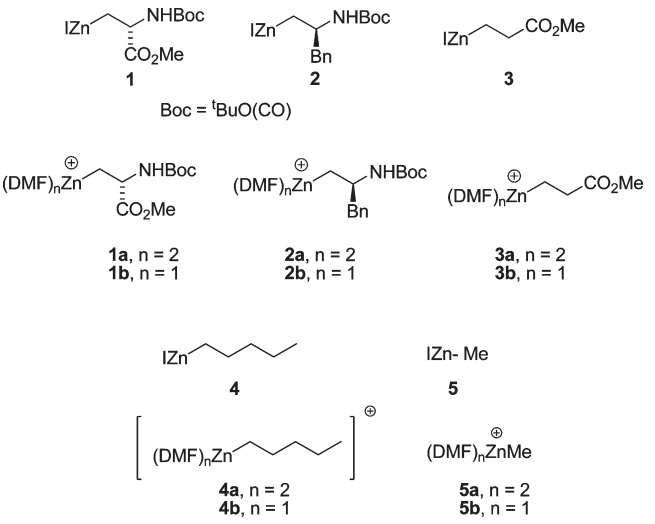


prepared by ESI have been reported.[20] However, ESI-MS and computational studies of zinc(II) complex ions with deprotonated carboxylic acid and/or amino acid ligands showed that the final desolvation step, i.e., the loss of the last solvent molecule, requires a substantially higher energy than the loss of previous solvent molecules. Consequently, isomerization reactions of the respective ligands are detected, which can compete with complete desolvation.[21−25] Here, alkylzinc-DMF complexes are sprayed from DMF solution and the derived complex ions are found with high abundance available for further examinations in the gas phase. To examine reliably the fragmentation patterns and to enable definitive structure assignments, exact ion masses of product and precursor species were determined in a hybrid linear ion trap/Orbitrap mass spectrometer.[26,27] In addition to the somewhat indirect probe of ion structures by interpretation of fragmentation reactions, it is attractive to use spectroscopic approaches, in particular infrared (IR) spectroscopy, as a more direct and definitive structural probe. Since direct IR spectroscopy of ions stored in an ion trap is not possible, the use of infrared multiple-photon dissociation (IRMPD) spectroscopy[28] has been developed as an effective "action spectroscopy"[29] alternative for the study

(6) Krasovskiy, A.; Duplais, C.; Lipshutz, B. H. *J. Am. Chem. Soc.* **2009**, *131*, 15592–15593.
(7) Duplais, C.; Krasovskiy, A.; Wattenberg, A.; Lipshutz, B. H. *Chem. Commun.* **2010**, 562–564.
(8) Duddu, R.; Eckhardt, M.; Furlong, M.; Knoess, H. P.; Berger, S.; Knochel, P. *Tetrahedron* **1994**, *50*, 2415–2432.
(9) Rilatt, I.; Caggiano, L.; Jackson, R. F. W. *Synlett* **2005**, 2701–2719.
(10) Caggiano, L.; Jackson, R. F. W.; Meijer, A. J. H. M.; Pickup, B. T.; Wilkinson, K. A. *Chem.—Eur. J.* **2008**, *14*, 8798–8802.
(11) Dexter, C. S.; Hunter, C.; Jackson, R. F. W.; Elliott, J. *J. Org. Chem.* **2000**, *65*, 7417–7421.
(12) Fenn, J. B.; Mann, M.; Meng, C. K.; Wong, S. F.; Whitehouse, C. M. *Science* **1989**, *246*, 64–71.
(13) Cole, R., Ed. *Electrospray Ionization Mass Spectrometry: Fundamentals, Instrumentation and Applications*; John Wiley & Sons: New York, 1997.
(14) Kebarle, P.; Verkerk, U. H. *Mass Spectrom. Rev.* **2009**, *28*, 898–917.
(15) Wells, J. M.; McLuckey, S. A. In *The Encyclopedia of Mass Spectrometry*; Gross, M. L., Caprioli, R., Eds.; Elsevier: New York, 2003; Vol. 1.
(16) di Marco, V. B.; Bombi, G. G. *Mass Spectrom. Rev.* **2006**, *25*, 347–379.
(17) Colton, R.; D'Agostino, A.; Traeger, J. C. *Mass Spectrom. Rev.* **1995**, *14*, 79–106.
(18) Schalley, C. A. *Mass Spectrom. Rev.* **2002**, *20*, 253–309.
(19) Schalley, C. A. *Int. J. Mass Spectrom.* **2000**, *194*, 11–39.
(20) Koszinowski, K.; Böhrer, P. *Organometallics* **2009**, *28*, 771–779. Fleckenstein, J. E.; Koszinowski, K. *Chem.—Eur. J.* **2009**, *15*, 12745–12753.
(21) Rogalewicz, F.; Louazel, G.; Hoppilliard, Y.; Ohanessian, G. *Int. J. Mass Spectrom.* **2003**, *228*, 779–795.
(22) Rogalewicz, F.; Hoppilliard, Y.; Ohanessian, G. *Int. J. Mass Spectrom.* **2000**, *201*, 307–320.
(23) Hoppilliard, Y.; Rogalewicz, F.; Ohanessian, G. *Int. J. Mass Spectrom.* **2001**, *204*, 267–280.
(24) Rogalewicz, F.; Hoppilliard, Y.; Ohanessian, G. *Int. J. Mass Spectrom.* **2001**, *206*, 45–52. Rogalewicz, F.; Hoppilliard, Y.; Ohanessian, G. *Int. J. Mass Spectrom.* **2003**, *227*, 439–451.
(25) Duchackova, L.; Roithova, J. *Chem.—Eur. J.* **2009**, *15*, 13399–13405.
(26) (a) Makarov, A.; Denisov, E.; Kholomeev, A.; Balschun, W.; Lange, O.; Strupat, K.; Horning, S. *Anal. Chem.* **2006**, *78*, 2113–2120. (b) Makarov, A. *Anal. Chem.* **2000**, *72*, 1156–1162.
(27) Schwartz, J. C.; Senko, M. W.; Syka, J. E. P. *J. Am. Soc. Mass Spectrom.* **2002**, *13*, 659–669.
(28) Bagratashvili, V. N.; Letokov, V. S.; Makarov, A. A.; Ryabov, E. A. *Multiple Photon Infrared Laser Photophysics and Photochemistry*; Harwood: Chichester, UK, 1985.
(29) Wing, W. H.; Ruff, G. A.; Lamb, J. W. E.; Spezeski, J. J. *Phys. Rev. Lett.* **1976**, *36*, 1488–1491.
(30) Duncan, M. A. *Int. J. Mass Spectrom.* **2008**, *272*, 99–118.
(31) Walker, N. R.; Walters, R. S.; Duncan, M. A. *New J. Chem.* **2005**, *29*, 1495–1503.

of a number of metal−ligand complexes in the gas phase.[30−42] IRMPD relies on the resonant noncoherent absorption of tens to hundreds of photons to reach internal energies where one or more dissociation pathways are usually accessible, and for which powerful laser systems are essential.[40] Free electron lasers (FEL) have proved to be well-suited for this task and have the capability of continuous wavelength-tunability over a very wide range (3−250 $\mu$m).[43] IRMPD spectra of each of the alkylzinc ions acquired are then related to computed IR spectra of gas phase ion structures identified and optimized by high-level DFT calculations.

## Results and Discussion

Organozinc iodides derived from naturally occurring α-amino acids have found widespread use in the stereocontrolled synthesis of non-natural analogues of proteinogenic amino acids (α-, $\beta$-, and $\gamma$-amino acid derivatives) without loss of stereochemical integrity.[9] In particular, serine-based reagent **1** (Scheme 1) has been widely used for the synthesis of α-amino acids.[9] Additionally, less functionalized organozinc iodides, specifically compounds containing a *tert*-butyloxycarbonyl-(Boc)-protected amino group **2**, an ester group **3**, or just an alkyl group (pentyl and methyl: compounds **4** and **5**, respectively) have been examined. This selection of alkylzinc compounds allows a study of the influence of these functional groups on the coordination sphere of zinc, complex stability, and may shed some light on the structure of these reagents (Scheme 1). Examination of solutions of alkylzinc iodides **1**−**5** in dry dimethylformamide by electrospray ionization has allowed the full characterization of the solvated cations **1b**, **2b**, **3a**, **3b**, **4a**, and **5a** formed by formal loss of $I^-$ in the gas phase. This set of ions proved to be sufficiently stable to serve as precursor ions for detailed MS/MS analysis, exact ion mass measurements, and IRMPD spectroscopy. As each of these gas phase organozinc ions is solvated by either one or two DMF molecules, they are certainly related to the actual species in DMF solution.

The divalent cation of zinc $Zn^{2+}$ possesses five doubly occupied 3d orbitals.[44] This closed shell $d^{10}$ configuration of the $Zn^{2+}$ dication explains its inertness to redox reactions and hence rationalizes the limited catalytic activity of Zn in proteins, as for example in carbonic anhydrase.[45] However, $Zn^{2+}$ has a vacant 4s orbital and is thereby a soft Lewis acid, which allows strong interaction with a variety of donor ligands, including sulfur from cysteine, nitrogen from histidine, and oxygen from glutamate, aspartate, or water. Another consequence of the filled 3d shell is the high preference for $Zn^{2+}$ to form tetrahedral complexes with four ligands leading formally to the [Kr] electron configuration. Tetrahedral $Zn^{2+}$ complexes are also found in a variety of protein complexes.[39,46−50] A tetrahedral template was therefore considered for the gross ion structures of the set of alkylzinc DMF cluster ions, e.g., ions **1b**, **2b**, and **3a** in Scheme 1.

**SCHEME 2. The ESI-MS Spectrum of Serine-Derived Compound 1 Exhibits the Alkylzinc-DMF Cluster Ions 1a at *m*/*z* 412 and 1b at *m*/*z* 339**[a]

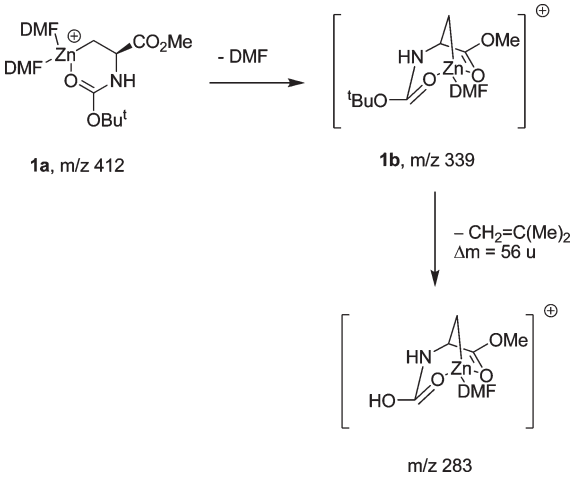


[a]The compositions of the ion **1b** $[C_{12}H_{23}N_2O_5{}^{64}Zn]^+$ and of the main CID and IRMPD product ion at *m*/*z* 283 $[C_8H_{15}O_5N_2{}^{64}Zn]^+$ are consistent with determined accurate ion masses, thereby confirming the loss of isobutene (see the Supporting Information, Figure 1S).

**Serine-Derived Alkylzinc Bis-DMF Adduct Ion 1a and Mono-DMF Analogue 1b.** The ESI-MS examination of alkylzinc iodide **1** yielded two characteristic alkylzinc-DMF cluster ions **1a** at *m*/*z* 412 and **1b** at *m*/*z* 339. The bis-DMF adduct ion **1a** exhibits a facile and exclusive loss of a DMF ligand to give the mono-DMF alkylzinc ion **1b** upon low-energy collision activation (Scheme 2). The calculated dissociation energy for this DMF (**1a** to **1b**) is 79.8 kJ/mol. The DMF cluster ion **1a** had not previously been detected, and its existence provides indirect evidence that the precursor alkylzinc iodide **1** also has (at least) two associated DMF molecules. Due to the substantially greater stability of ion **1b** its fragmentation behavior could be examined by CID (see Scheme 3). The loss of methyl acrylate from the ion at *m*/*z* 283 is a very close mirror of the corresponding solution phase elimination reaction of $\beta$-amino alkylzinc iodides that has previously been studied.[11] As the sequential fragmentation reactions shown in Scheme 3 illustrate, the remaining DMF ligand is retained throughout the activation events while parts of the organic ligand are lost by sequential cleavage of

(32) Duncan, M. A. *Int. J. Mass Spectrom.* **2000**, *200*, 545–569.
(33) Oomens, J.; Moore, D. T.; von Helden, G.; Meijer, G.; Dunbar, R. C. *J. Am. Chem. Soc.* **2004**, *126*, 724–725.
(34) Cabarcos, O. M.; Weinheimer, C. J.; Lisy, J. M. *J. Chem. Phys.* **1999**, *110*, 8429–8435.
(35) Moore, D. T.; Oomens, J.; Eyler, J. R.; Meijer, G.; von Helden, G.; Ridge, D. P. *J. Am. Chem. Soc.* **2004**, *126*, 14726–14727.
(36) Kapota, C.; Lemaire, J.; Maitre, P.; Ohanessian, G. *J. Am. Chem. Soc.* **2004**, *126*, 1836–1842.
(37) Polfer, N.; Paizs, B.; Snoek, L. C.; Compagnon, I.; Suhai, S.; Meijer, G.; von Helden, G.; Oomens, J. *J. Am. Chem. Soc.* **2005**, *127*, 8571–8579.
(38) Moore, D. T.; Oomens, J.; Eyler, J. R.; von Helden, G.; Meijer, G.; Dunbar, R. C. *J. Am. Chem. Soc.* **2005**, *127*, 7243–7254.
(39) Polfer, N.; Oomens, J.; Moore, D. T.; von Helden, G.; Meijer, G.; Dunbar, R. C. *J. Am. Chem. Soc.* **2006**, *128*, 517–525.
(40) Polfer, N.; Oomens, J. *Mass Spectrom. Rev.* **2009**, *28*, 468–494.
(41) Fridgen, T. D. *Mass Spectrom. Rev.* **2009**, *28*, 586–607.
(42) Bakker, J. M.; Besson, T.; Lemaire, J.; Scuderi, D.; Maitre, P. *J. Phys. Chem. A* **2007**, *111*, 13415–13424.
(43) Oepts, D.; van der Meer, A. F. G.; van Amersfoort, P. W. *Infrared Phys. Technol.* **1995**, *36*, 297–308.
(44) Prince, R. H. *Adv. Inorg. Radiochem.* **1979**, *22*, 349–440.
(45) Winum, J.-Y.; Scozzafava, A.; Montero, J.-L.; Supuran, C. T. *Curr. Top. Med. Chem.* **2007**, *7*, 835–848.
(46) Berg, J. M.; Shi, Y. *Science* **1996**, *271*, 1081–1085.
(47) Regan, L.; Clarke, N. D. *Biochemistry* **1990**, *29*, 10878–10883.
(48) Klemba, M.; Regan, L. *Biochemistry* **1995**, *34*, 10094–11010.
(49) Venkataraman, D.; Du, Y.; Wilson, S. R.; Hirsch, K. A.; Zhang, P.; Moore, J. S. *J. Chem. Educ.* **1997**, *74*, 915–918.
(50) Berg, J. M.; Merkle, D. L. *J. Am. Chem. Soc.* **1989**, *111*, 3759–3761.

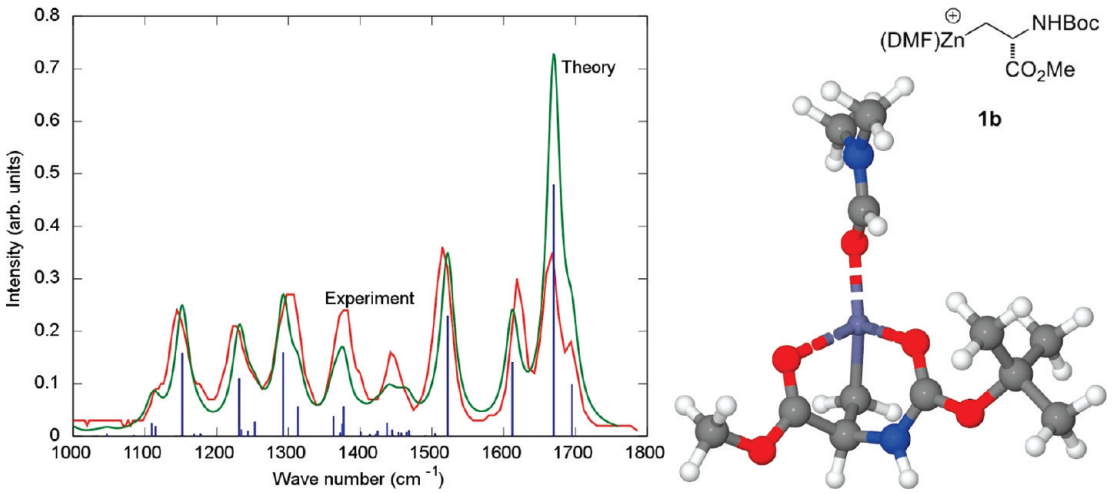


**FIGURE 1.** IRMPD and calculated IR spectrum of alkylzinc-DMF cluster ion **1b** at *m*/*z* 339. The depicted ion structure was identified by theory to be the most stable gas phase structure.

**SCHEME 3. Fragmentation Reactions of the Alkylzinc-DMF Cluster Ion 1b at *m*/*z* 339 upon CID in an Octapole**[a]

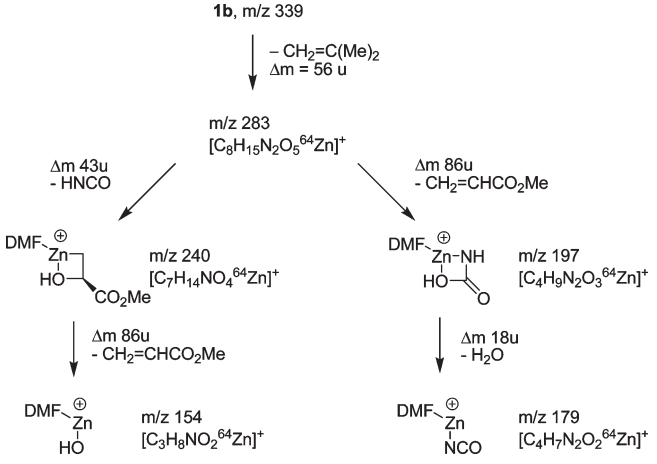


[a]The depicted ion structures are indicative and are consistent with determined accurate ion masses.

covalent bonds.[21] The calculated dissociation energy for the DMF molecule in cation **1b** is 186.1 kJ/mol, explaining why it is not lost.

For the alkylzinc-DMF cluster ion **1b** at *m*/*z* 339 a single minimum structure was identified by calculation, featuring internal coordination of zinc by the carbonyl oxygen atoms of the ester group, the carbamate of the Boc protecting group, and the coordinated DMF (see the structure in Figure 1). In this structure, which is computed to be the most stable conformer for **1b**, the zinc ion adopts tetrahedral coordination geometry, typical for zinc complexes with 4 ligands.[46–50]

In Figure 1, the IRMPD spectrum of the alkylzinc-DMF cluster ion **1b** is compared to the calculated IR spectrum of the lowest energy conformer identified by theory (see inserted structure). The IR spectrum of the depicted structure of ion **1b** shows quite clearly a quantitative agreement with the experimental data. All major features of the recorded IRMPD spectrum of **1b** are consistent with the absorption spectrum of the low energy ion structure of **1b**, which is included in Figure 1. The IRMPD spectrum of **1b** contains a rich pattern of at least eight well-resolved signals in the range of 1100−1700 $cm^{-1}$. Characteristic absorptions are found between 1500 and 1600 $cm^{-1}$, where the C−N bonds of the DMF and the Boc-protected amino functionality of the identified structure of **1b** absorb strongly. The characteristic C═O stretching modes of the three carbonyl chromophores are found higher than 1600 $cm^{-1}$.[34–39] The calculated intensity of the DMF carbonyl mode appears overestimated by theory (1670 $cm^{-1}$ band). This may be related to the fact that DFT does not evaluate van der Waals forces correctly, which has often led to discrepancies between computed and actual intensities as well as frequencies.[37,39,41,51,52] In the case of the ion **1b**, the description of the interaction of the DMF carbonyl with zinc seems to be especially sensitive to this problem. The exaggerated intensities of the band at 1670 $cm^{-1}$ persist in noncounterpoise corrected calculations and are therefore not due to the counterpoise correction. Additional B3LYP calculations were carried out at the noncounterpoise level, using both bigger (6311G** on all atoms) and smaller basis sets (SDD keyword in Gaussian03) than the one specified in the Experimental Section. In addition, an MP2 calculation was carried out with use of the latter basis set, since our resources did not allow us to perform frequency calculations for the larger basis sets. From these calculations it can be concluded that MP2 may give better intensities for the basis set specified in the Experimental Section. However, there is also clearly a basis set effect and our present resources do not allow these two effects to be disentangled. Finally, it should also be noted that the multiple photon excitation mechanism may perturb intensities from what would have been observed in a linear absorption spectrum.[53]

Nevertheless, in spite of the exaggerated intensities of the band at 1670 $cm^{-1}$, the otherwise excellent agreement of the experimental and calculated spectrum of **1b** allows for a convincing structural assignment.

(51) Drayss, M. K.; Blunk, D.; Oomens, J.; Polfer, N.; Schmuck, C.; Gao, B.; Wyttenbach, T.; Bowers, M. T.; Schäfer, M. *Int. J. Mass Spectrom.* **2009**, *281*, 97–100.
(52) Halls, M. D.; Schlegel, H. B. *J. Chem. Phys.* **1998**, *109*, 10587–10593.
(53) Oomens, J.; Sartakov, B. G.; Meijer, G.; von Helden, G. *Int. J. Mass Spectrom.* **2006**, *254*, 1–19.

**SCHEME 4. Fragmentation Reactions Found in the QIT-MS$^2$ Product Ion Spectrum of 2b at *m/z* 371**[a]

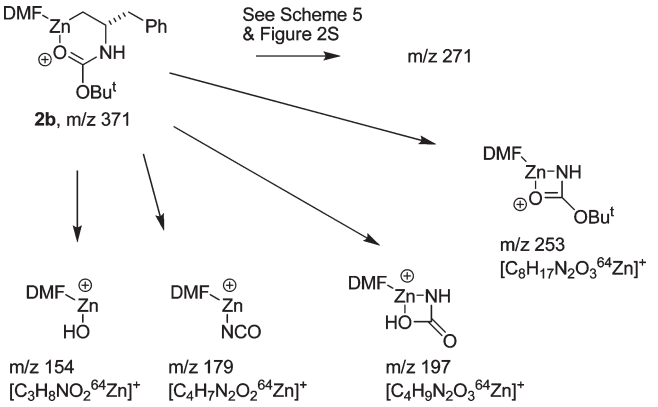


[a]The depicted ion structures are indicative and the formulae are consistent with accurate ion masses determined.

**Alkylzinc Bis-DMF Adduct Ion 2a and Mono-DMF Analogue 2b.** Results of the ESI-MS and the CID experiments of compound **2** are comparable to the results obtained for compound **1**. Alkylzinc-DMF cluster ions derived from **2** with either two DMF molecules (at *m/z* 444: **2a**) or with one DMF molecule (at *m/z* 371: **2b**) are found in the gas phase. Bis-DMF adduct ion **2a** is not stable enough to be isolated and separately stored in an ion trap, as it instantly loses a DMF molecule upon slight collision activation (the calculated dissociation energy for this DMF is 94.6 kJ/mol). The remaining DMF ligand in **2b** is strongly bound (calculated dissociation energy 164.1 kJ/mol), and is retained upon CID (see Schemes 4 and 5). As already observed in the CID of cation **1b**, the alkylzinc mono-DMF ion **2b** possesses a very strong bond between the DMF carbonyl oxygen and the zinc ion, which proves to be substantially stronger than covalent bonds in the molecule (cf. Scheme 3). In CID experiments of **2b** an interesting fragmentation reaction involving a ligand displacement reaction is postulated to explain the formation of the product ion at *m/z* 271 (see Schemes 4 and 5 and in the Supporting Information Figure 2S).[54−59] As illustrated in Scheme 5 the mass difference measured ($\Delta m$ = 100.0678 u) implies the neutral loss of $C_9H_{10}$ (3-phenylpropene) combined with an addition of $H_2O$ ($\Delta m(C_9H_{10} - H_2O)$ = 100.0677 u). The product ion matches the measured value perfectly (ion mass $[C_8H_{19}N_2O_4{}^{64}Zn]^+$ (calculated) 271.06308 u, (measured) = 271.0631 u). A similar fragmentation reaction is also postulated to explain the CID behavior of **3b** (see Scheme 1S in the Supporting Information).[54−59] The origin of the $H_2O$ in the ion trap available for addition in the gas phase is to be further examined.

For the alkylzinc-DMF cluster ion **2b** a set of six conformers was computationally identified (Figure 2). All of these gas phase structures of **2b** feature internal coordination of zinc by the carbonyl oxygen atoms of the carbamate protecting group and DMF (see Figure 2). Structure a in Figure 2 is predicted to be the global minimum structure of **2b** by DFT (0.0 kJ/mol). However, the one-but-lowest energy conformer (structure b in Figure 2; at 2.28 kJ/mol) clearly shows the best agreement with the acquired IRMPD spectrum of **2b**, as Figure 3 demonstrates (Discussion, see below). Conformer b is the most compact of the six structures identified, showing an additional side-on interaction between zinc and the slightly bent phenyl $\pi$-system, an example of the well-known cation$-\pi$ interaction.[60] The coordination geometry around zinc in this structure can be considered to be at least roughly tetrahedral (Figure 2).[46−50] It is reasonable to suggest that the phenyl ring may play a role in promoting the loss of DMF from the cluster ion **2a**. Probably as a result of the poor description of van der Waals forces in DFT, structure b in Figure 2 is not found to be the lowest energy conformer, rendering the more direct interaction in structure a lower in energy than the side-on interaction in structure b. To test this hypothesis these molecules were reoptimized by using second-order Moller−Plesset perturbation theory (MP2) (ignoring BSSE corrections in this particular case). Structure b in Figure 2 is now lower in energy than structure a by 34.1 kJ/mol at the MP2 level of theory. It should be pointed out that MP2 will overestimate van der Waals interactions and that the actual energy difference between the two structures will be smaller.

**SCHEME 5. The Exact Ion Masses of 2b, i.e., the Precursor Ion at *m/z* 371, and of Its CID Product Ion at *m/z* 271 Were Accurately Determined and the Neutral Loss of 100 u Was Precisely Derived**[54−59]

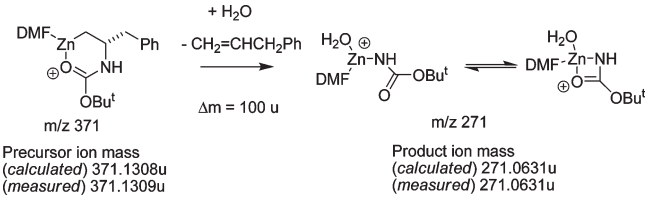


In Figure 3, the IRMPD spectrum of the alkylzinc-DMF cluster ion **2b** is compared to the calculated IR spectra of the six conformers identified by theory (Figure 2). The well-resolved IRMPD spectrum of **2b** exhibits at least ten absorption bands in the 1100−1700 cm$^{-1}$ range. All major and minor features in the IRMPD spectrum of **2b** are consistent with the computed spectrum of conformer b, which reproduces the experimental spectrum of **2b** substantially better than any of the other conformers does. The structure assignment is based on the very good match of the several low and medium intensity bands below 1500 cm$^{-1}$ and the three major absorptions above 1500 cm$^{-1}$. In the latter range, we observe the two characteristic C=O stretching modes of the carbonyl chromophores and C−N bending mode of the Boc-protected amine. The decisive band is located at about 1620 cm$^{-1}$, which can be attributed to the strong carbonyl stretch of the carbamate carbonyl group and the bending modes of the phenyl ring of **2b** (this particular mode is illustrated in an animated presentation in the Supporting Information). The presence of the cation$-\pi$ interaction of the zinc metal ion

(54) Thevis, M.; Kohler, M.; Schlörer, N.; Schänzer, W. *J. Am. Soc. Mass Spectrom.* **2008**, *19*, 151–158.
(55) Beuck, S.; Schwabe, T.; Grimme, S.; Schlörer, N.; Kamber, M.; Schänzer, W.; Thevis, M. *J. Am. Soc. Mass Spectrom.* **2009**, *20*, 2034–2048.
(56) Weisz, A.; Andrzejewski, D.; Fales, H. M.; Mandelbaum, A. *J. Mass Spectrom.* **2002**, *37*, 1025–1033.
(57) Perera, B. A; Ince, M. P.; Talaty, E. R.; Van Stipdonk, M. J. *Rapid Commun. Mass Spectrom.* **2001**, *15*, 615–622.
(58) Kölliker, S; Oehme, M; Merz, L. *Rapid Commun. Mass Spectrom.* **2001**, *15*, 2117–2126.
(59) Guan, Z.; Liesch, J. M. *J. Mass Spectrom.* **2001**, *36*, 264–276.
(60) Ma, J. C.; Dougherty, D. A. *Chem. Rev.* **1997**, *97*, 1303–1324.

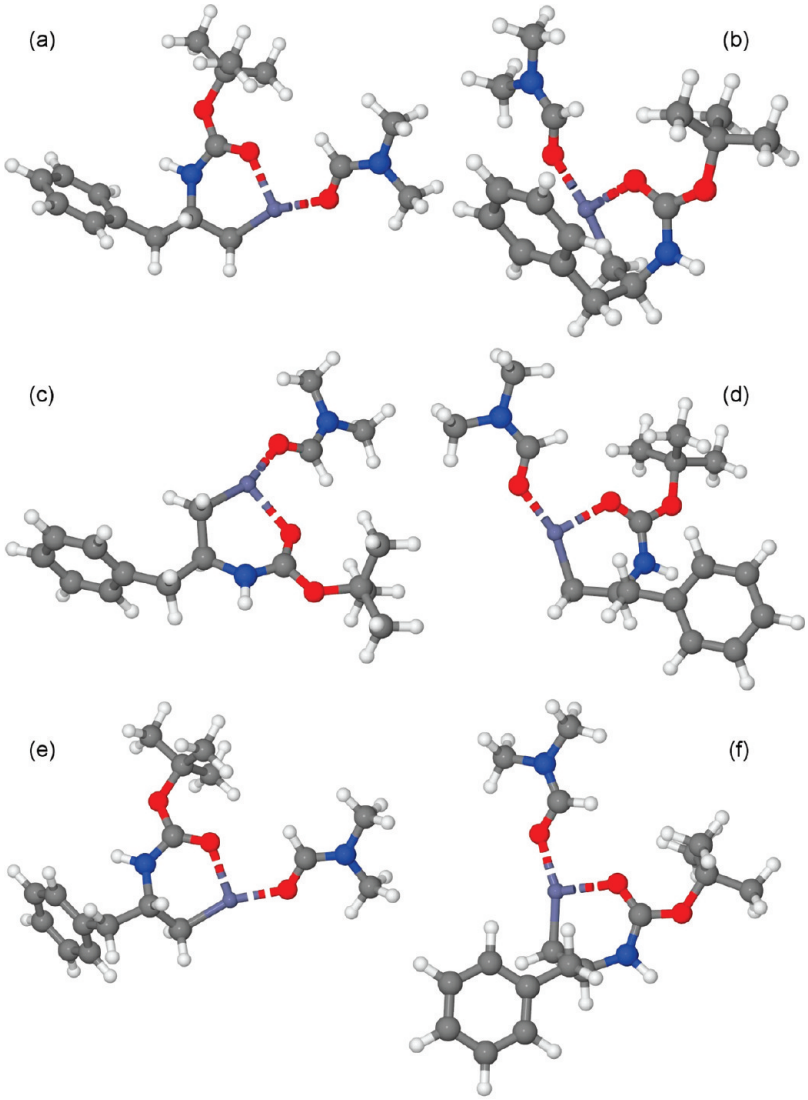


**FIGURE 2.** Six lowest energy conformers for the phenyl-based compound **2b**. All energies and geometries are corrected for BSSE. Relative energies found by DFT of the structures were (a) 0.0, (b) 2.28, (c) 6.06, (d) 6.38, (e) 7.23, and (f) 9.60 kJ/mol.

with the phenyl group clearly present in structure b of **2b** offers a straightforward explanation for the comparatively good match with the composite signal found experimentally at 1620 $cm^{-1}$. This interaction is only present in conformer b of **2b** and absent in all five other conformers. In conclusion, good overall agreement of the experimental with the calculated spectrum of the identified conformer of **2b** allows a convincing assignment of the structure.

**Alkylzinc Bis-DMF Adduct Ion 3a and Mono-DMF Analogue 3b.** As organozinc iodide **3** does not incorporate any coordination site for zinc other than the ester oxygen, the bis-DMF cluster ion **3a** at *m*/*z* 297 was found to be substantially more stable than the corresponding bis-DMF adduct ions **1a** and **2a**, probably a result of the competition of internal coordination sites with additional DMF solvent molecules. This behavior is entirely consistent in each case with the preferred formation of a tetrahedral four-coordinate zinc cation, from which loss of one molecule of DMF is possible.[10] The bis-DMF cluster ion **3a** could be selected, isolated, and further examined by IRMPD and CID. In the CID product ion spectrum of ion **3a** (see Figure 3S and Scheme 1S in the Supporting Information) the exclusive loss of DMF is observed (calculated dissociation energy for **3a** to **3b** is 103.6 kJ/mol), whereas in the subsequent $MS^3$ product ion spectrum of **3b** at *m*/*z* 224 the loss of the remaining DMF molecule and the addition of water was detected.[54−59]

For the bis-DMF cluster ion **3a** at *m*/*z* 297 a set of three conformers was identified by DFT (Figure 4S in the Supporting Information). Each of the gas phase structures identified for **3a** features coordination of zinc by the carbonyl oxygen atom of the ester and the DMF molecules. Structure a in Figure 4S (Supporting Information) was predicted to be the global minimum structure of **3a** (0.0 kJ/mol). For the mono-DMF analogue ion **3b** at *m*/*z* 224 only a single conformer was identified by calculation (see Figure 5). In the calculated spectrum of the ion **3a** the three carbonyl stretching modes combine to produce a broad feature at the blue end of the scale (1640−1710 $cm^{-1}$), whereas in the mono-DMF adduct ion **3b**, the strong absorptions of the carbonyl chromophores of the ester and the DMF interfere and deliver a partly resolved signal at 1640−1680 $cm^{-1}$. In both cases the experimental

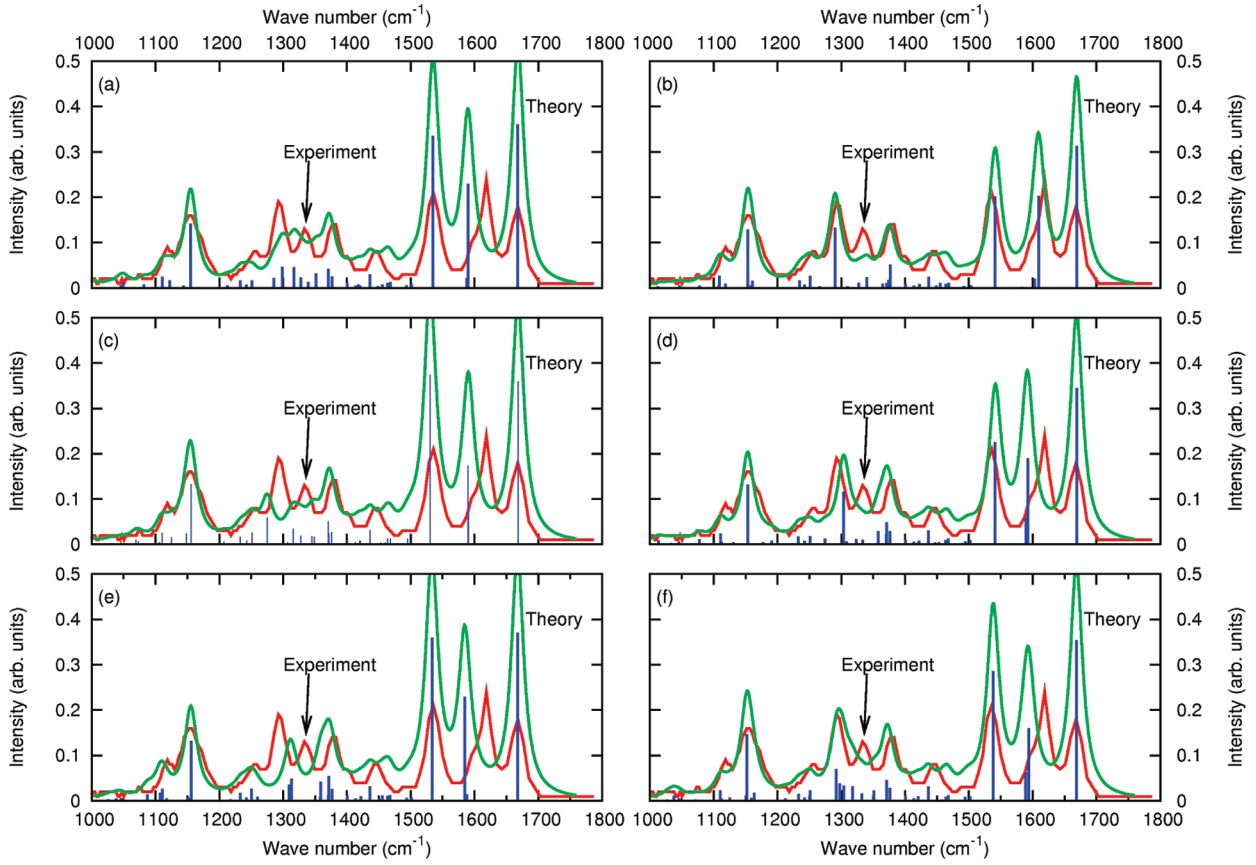


**FIGURE 3.** IRMPD spectra (green) generated for the six lowest energy conformers for the phenyl zinc-DMF cluster ion **2b** compared to the recorded IRMPD spectrum of **2b** (red). The structures are labeled according to Figure 2. The one-but-lowest energy conformer (structure b in Figure 2 at 2.28 kJ/mol relative energy) clearly exhibits the best agreement with the recorded spectrum of **2b**.

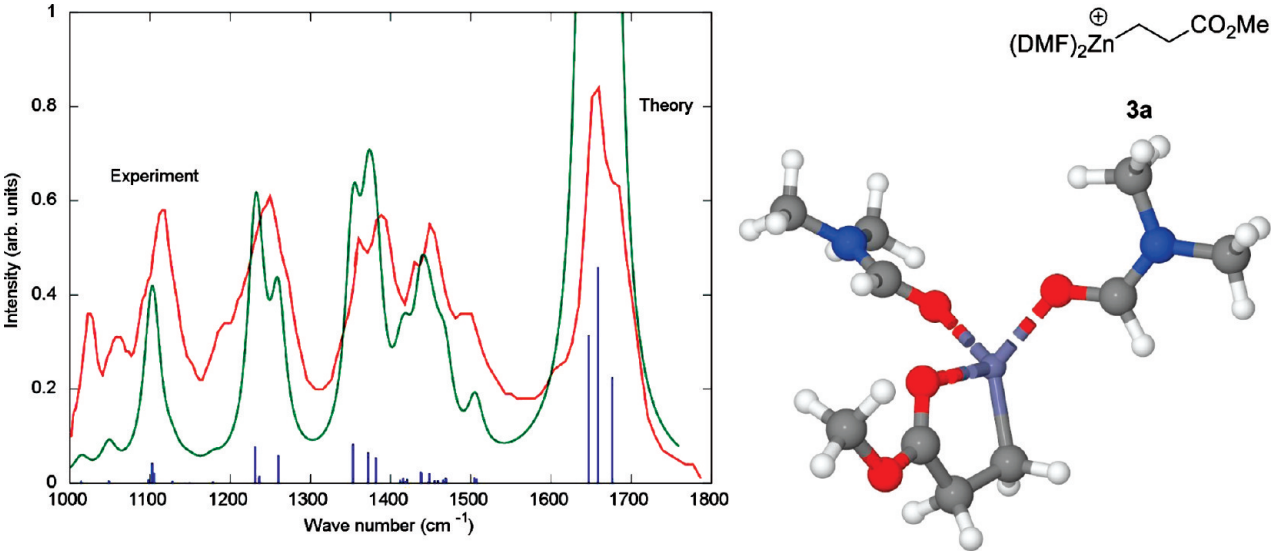


**FIGURE 4.** IRMPD and calculated IR spectrum of the bis-DMF cluster ion **3a** at *m*/*z* 297 with 2 DMF molecules attached to zinc. The depicted tetrahedral ion structure was identified by theory to be the most stable gas phase structure (see structure a in Figure 4S).

spectrum is convincingly reproduced by the absorptions of the structures identified by theory (Figures 4 and 5). The calculated structures for **3a** are very similar, with energies within kT of each other, and the calculated IR spectra of each of the three conformers of **3a** are also very similar (see Figure 5S in the Supporting Information). One can conclude that the conformers of **3a** need not be distinguished. We note a substantial discrepancy between the measured and the calculated intensity of the three interfering carbonyl stretching modes of the conformers of **3a** illustrated in Figure 5S (Supporting Information), and as already noted in the case of **1b**.[37,39,41,51,52]

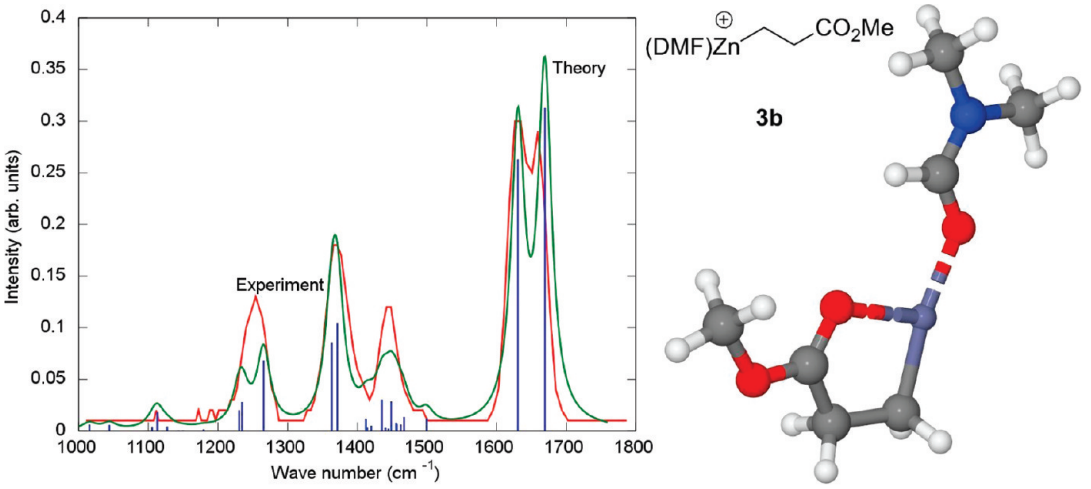


**FIGURE 5.** IRMPD and calculated IR spectrum of the cluster ion **3b** at *m*/*z* 224 with a single DMF molecule attached. The depicted ion structure was the only relevant gas phase structure of **3b** identified by theory.

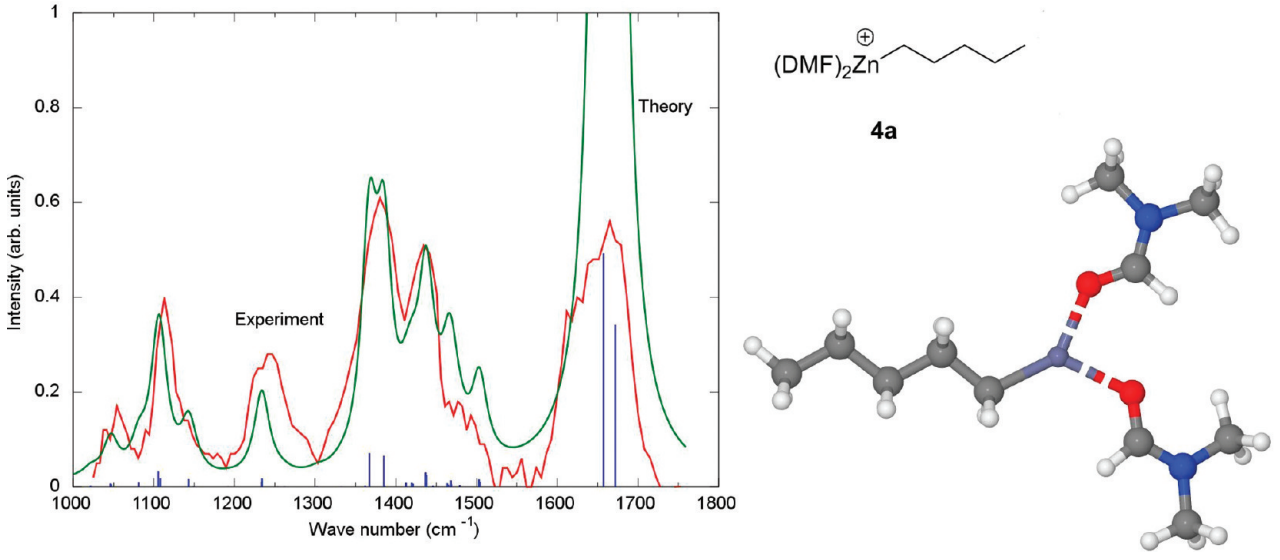


**FIGURE 6.** IRMPD and calculated IR spectrum of pentylzinc-bis-DMF cluster ion **4a** at *m*/*z* 281. The depicted ion structure was identified by theory to be the most stable gas phase structure.

**Unfunctionalized Pentylzinc Bis-DMF Ion 4a and Methylzinc Bis-DMF Ion 5a.** Finally, the behavior of each of the simple unfunctionalized alkylzinc iodides **4** and **5** was investigated by ESI-MS. Jackson et al. succeeded in generating the pentylzinc tris-DMF complex ion at *m*/*z* 354,[10] which could not be observed in the present ESI-MS experiments even under the mildest ESI conditions possible. The formation of a pentylzinc tris-DMF complex ion was initially expected, since this would follow the general pattern that tetrahedral complex ions of cationic zinc with four ligands are favored.[10] Nevertheless, the calculated dissociation energies for the loss of DMF from each of the tris-DMF complexes to give the corresponding bis-DMF complexes **4a** and **5a** were calculated to be 85.5 and 88.7 kJ/mol, respectively, explaining their instability. Under very mild ionization conditions only the pentylzinc bis-DMF adduct ion **4a** at *m*/*z* 281 and the corresponding methylzinc derivative **5a** at *m*/*z* 225 could be isolated for further gas phase investigations. It is very likely that the heated transfer capillary hold at $T = 230$ °C, which is needed for complete and effective desolvation through convection, results in loss of a DMF molecule in the transfer region of the ion source used, thereby depleting any alkylzinc tris-DMF complex ion population that might have formed.

Product ion experiments by CID of **4a** and **5a** yielded only the loss of a DMF molecule ($\Delta m = 73$ u) to give the cations **4b** and **5b** (the dissociation energies were calculated to be 120.2 and 128.2 kJ/mol, respectively). The overall intensities of the mono-DMF adduct ions **4b** and **5b** were too small for further CID investigations in $MS^3$ product ion experiments.

Ions **4a** and **5a** were further investigated by IRMPD spectroscopy. For the pentylzinc bis-DMF adduct ion **4a** at *m*/*z* 281 a set of three conformers was found by DFT (Figure 6S in the Supporting Information). All three gas phase conformers of **4a** exhibit coordination of zinc to the carbonyl oxygens of each DMF molecule, and are within kT of each other in energy. Structure a in Figure 6S is predicted to be the global minimum structure of **4a** (0.0 kJ/mol) and the

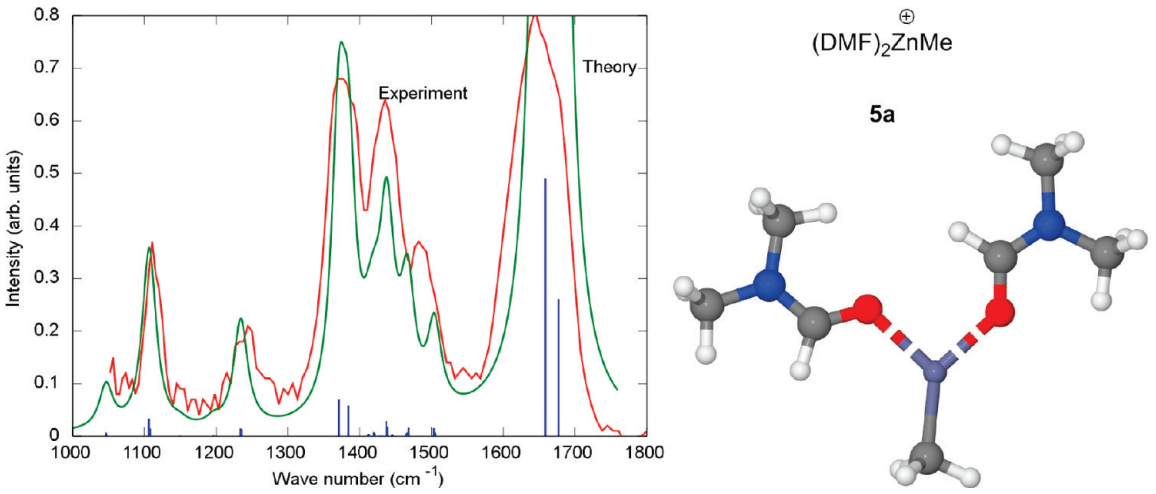


**FIGURE 7.** IRMPD and calculated IR spectrum of methylzinc-bis-DMF cluster ion **5a** at *m*/*z* 225. The depicted ion structure was identified by theory to be the most stable gas phase structure.

corresponding computed IR-spectrum matches the recorded spectrum of **4a** (Figure 6). For the methyl zinc bis-DMF analogue ion **5a** at *m*/*z* 225 only a single conformer was identified by theory (see Figure 7). In the calculated spectrum of the ion **4a** the stretching modes of the two DMF carbonyls combine to form to a broad feature at the blue end of the scale (1600−1700 $cm^{-1}$). An analogous spectral pattern is found for the methylzinc bis-DMF ion **5a** at *m*/*z* 225 (Figure 7). In both cases the experimental spectrum is convincingly reproduced by the absorptions of the structures identified by theory (Figures 6 and 7). However, all conformers of **4a** identified by theory deliver almost identical IR spectra, which are depicted in Figure 7S of the Supporting Information. One can conclude that the conformers of **4a** need not be distinguished, as already noted in the case of the energetically close conformers of **3a**.

## Conclusions

An extended series of alkylzinc-DMF cluster ions was investigated for the first time by a combination of ESI-MS/MS, accurate ion mass measurements, and photodissociation spectroscopy, and augmented by computational methods. The zinc cation in gas phase alkylzinc-DMF species adopts preferably a tetrahedral coordination sphere with four ligands, namely the alkyl group, any internal coordinating groups, and DMF (the number of which depends on the number of internal coordinating groups present).[10] Under more energetic ion source conditions or induced by collision activation, sequential loss of coordinated DMF occurs, although it becomes progressively harder. According to our calculations, it appears that DMF-solvated cations in which the dissociation energy of one of the DMF molecules is less than approximately 100 kJ/mol are too unstable to be studied under the conditions of our experiments, whereas analogous cations for which DMF dissociation energies are all greater than this apparent lower limit can be directly studied. In the series of the analytes investigated the ester compound **3** exemplifies this general trend. Compound **3** does not offer any other coordination site for zinc than the oxygens of the ester moiety, so the corresponding four-coordinate bis-DMF cluster ion **3a** is found to be substantially more stable than the analogous bis-DMF adduct ions **1a** and **2a**, in which internal coordination competes with complexation of zinc by DMF. Consequently, the functionalized compounds **1** and **2** produce mono-DMF adduct ions, which are more stable than the corresponding bis-DMF ions. The calculated structures of the neutral reagents **1**−**5** in DMF solution show that zinc can be coordinated to at least two DMF molecules.[10] The results reported here suggest that in the course of the phase transfer from DMF solution to the gas phase by ESI, during which loss of the iodide ion occurs, the coordinated DMF molecules that are originally coordinated to zinc can be displaced by internal ligands (e.g., carbamate, ester or phenyl ring) if present.

The CID fragmentation patterns clearly demonstrate that the zinc-DMF interaction in tetrahedral four-coordinate zinc complex ions is of pronounced strength as the DMF molecule is retained while covalent bonds in the organic fragment dissociate.

Relevant gas phase structures of the series of alkylzinc-DMF cluster ions have been identified by high-level computations and the corresponding IR spectra have been calculated. These computed IR spectra match the acquired photodissociation spectra strikingly well, allowing convincing identification and assignment of the gas phase ion structures predicted by theory. Furthermore, our studies have allowed an exploration of the features of the identified ion structures in detail. The DMF adduct ions examined in the gas phase adopt preferably a tetrahedral coordination sphere around the zinc cation. Additionally, we find ample experimental evidence for the pronounced strength of the zinc−DMF bond in **1b** and **2b**, which survives even multiple collision activation processes and persists in daughter ions; this observation is entirely consistent with the calculated DMF dissociation energies.

The extent to which the easy ionization of the zinc−iodine bond of alkylzinc iodides in DMF solution when subjected to mild electrospray conditions reflects the behavior of the reagents in solution remains to be established. Nevertheless, if this facilitated dissociation of the iodine−zinc bond promoted by coordinating solvents such as DMF and by the presence of internal coordinating groups occurs, the

resulting partial or substantial positive charge located on zinc provides a clear explanation for the lack of reactivity of these reagents toward electrophiles and the high functional group tolerance of alkylzinc iodides, especially toward protons, since the alkyl fragment would be less basic with a partial positive charge on zinc.

In conclusion, the results presented clearly show that the particular combination of sophisticated analytical and computational techniques is appropriate to examine the delicate balance between coordination of zinc in alkylzinc-DMF cluster ions either internally by functional groups within the organic fragment or externally by the noncovalently bound DMF solvent molecules.

## Experimental Section

**Materials.** Alkylzinc iodides **1**−**5** were synthesized according to a standard protocol described in detail elsewhere.[10] The alkylzinc reagents **1**−**5** were prepared as solutions in dry dimethylformamide, and then analyzed with use of ESI-MS in positive ion mode by direct injection without any special precautions.

**Mass Spectrometry.** Alkylzinc cluster ions **1a**, **1b**, **2a**, **2b**, **3a**, **3b**, **4a**, and **5a** are found in the gas phase after formal loss of the iodide anion and stabilization with $n$ DMF molecules ($n = 1, 2$) after phase transfer with ESI. For all ESI experiments aliquots of the alkylzinc iodide solutions were diluted with dry DMF and used directly (concn sub mM). It should be noted that the number of DMF solvent molecules associated with the alkylzinc cations found in the gas phase by ESI-MS depends on the ion source conditions and was individually optimized.[10] The collision induced dissociation (CID) experiments were performed in either the octapole located in front of a quadrupole ion trap (QIT) or the QIT itself of a Finnigan MAT 900 instrument with an EB-QIT configuration, equipped with an ESI-I ion source (ThermoFisher, Bremen, Germany). For all CID experiments performed either in the octapole or in the QIT, helium (ultra high purity, $O_2 < 0.01$ ppm, $H_2O < 0.02$ ppm; Air Products, Hattingen, Germany) was used as the collision gas. The helium used in the octapole leaks from the QIT and its pressure therefore cannot be controlled separately or accurately measured. Monoisotopic precursor ion selection was performed for all types of product ion CID experiments to avoid overlapping of the large isotopic signal patterns due to the presence of Zn. The lightest isotopologue was exclusively selected for all MS experiments by using the most abundant Zn isotope, i.e., $^{64}$Zn (and for $^{12}$C, $^{16}$O, $^{1}$H, and $^{14}$N). ESI-MS conditions: Flow rate 3 $\mu$L/min, no sheath gas, spray voltage 3.7 kV, and heated capillary temperature 230 °C. The exact ion mass measurements were conducted (external calibration; resolution > 20000 fwhm) on a LTQ-Orbitrap instrument (ThermoFisher) equipped with an ESI ion source. All exact ion masses were determined with an experimental error of ≤0.5 ppm.[26]

**Infrared Multiphoton Dissociation Spectroscopy.** A 4.7 T Fourier transform ion cyclotron resonance (FTICR) mass spectrometer was used for the IRMPD experiments and has been described in detail elsewhere.[39,53,61,62] Tunable radiation for the photodissociation experiments was generated by the free electron laser for infrared experiments (FELIX).[43] For the present experiments, spectra were recorded over the wavelength range from 1000 to 1800 cm$^{-1}$. Pulse energies were around 50 mJ per macropulse of 5 $\mu$s duration, although they fell off to about 20 mJ toward the blue edge of the scan range. The fwhm bandwidth of the laser was typically 0.5% of the central wavelength. Alkylzinc-DMF cluster ions were formed by electrospray ionization, using a Micromass Z-Spray source with diluted reaction solutions (concn sub mM) of the appropriate alkylzinc iodide in dry DMF. Solution flow rates ranged from 15 to 30 $\mu$L/min and the electrospray needle was generally held at a voltage of +3.2 kV. Ions were accumulated in a hexapole trap for about 2 s prior to being injected into the ICR cell via an rf octopole ion guide. Electrostatic switching of the dc bias of the octopole allows ions to be captured in the ICR cell without the use of a gas pulse, thus avoiding collisional heating of the ions.[62] All complex ions were irradiated for 3 s, corresponding to interaction with 15 macropulses.

The fragmentation reactions found in IRMPD of the alkylzinc DMF cluster ions **1a**, **1b**, **2a**, **2b**, **3a**, and **3b** were analogous to those found upon low-energy CID (see Figures 1S and 4S and Scheme 3S in the Supporting Information). Precursor ions **4a** and **5a** exhibited an exclusive loss of a DMF ligand upon either CID or IRMPD. The IRMPD spectra were recorded by monitoring the most abundant product ions and the depletion of the respective precursor ion over the 1000−1800 cm$^{-1}$ range. The IRMPD yield was determined from the precursor ($I_P$) intensity and the intensity of the product ions ($\sum I_{\text{product ions}}$) after laser irradiation at each frequency:

$$\text{IRMPD yield} = \sum I_{\text{productions}}/(I_P + \sum I_{\text{productions}}) \qquad (1)$$

The yield was normalized linearly with laser power to take account of the change in laser power as a function of photon energy.[63]

**Computational Methods.** All electronic structure calculations were performed with use of the SMP version of the Gaussian 03 program package[64] with the B3LYP functional method.[65] Gaussian was compiled using the Portland Compiler version 7.0-5 with the GOTO implementation (v.1.2.6) of BLAS[66] on the EMT64 architecture. In all calculations we used a Stuttgart/Dresden pseudopotential[67] on Zn/I and the 6-311G** basis set on all other atoms.[68] For each molecule a series of conformers was generated by placing DMF molecules in feasible positions around the zinc center, or near the NH proton of the carbamate (when present). All chemically obvious structures were submitted as input geometries for in vacuo optimization. From the optimized geometries with the lowest energies additional optimizations were performed, with corrections for basis set superposition error (BSSE) using the method due to Boys

(61) Polfer, N.; Oomens, J. *Phys. Chem. Chem. Phys.* **2007**, *9*, 3804–3817.
(62) Valle, J. J.; Eyler, J. R.; Oomens, J.; Moore, D. T.; van der Meer, A. F. G.; von Helden, G.; Meijer, G.; Hendrickson, C. L.; Marshall, A. G.; Blakney, G. T. *Rev. Sci. Instrum.* **2005**, *76*, 023103.
(63) Drayss, M. K.; Blunk, D.; Oomens, J.; Gao, B.; Wyttenbach, T.; Bowers, M. T.; Schäfer, M. *J. Phys. Chem. A* **2009**, *113*, 9543–9550.
(64) Frisch, M. J.; Trucks, G. W.; Schlegel, H. B.; Scuseria, G. E.; Robb, M. A.; Cheeseman, J. R.; Montgomery, Jr., J. A.; Vreven, T.; Kudin, K. N.; Burant, J. C.; Millam, J. M.; Iyengar, S. S.; Tomasi, J.; Barone, V.; Mennucci, B.; Cossi, M.; Scalmani, G.; Rega, N.; Petersson, G. A.; Nakatsuji, H.; Hada, M.; Ehara, M.; Toyota, K.; Fukuda, R.; Hasegawa, J.; Ishida, M.; Nakajima, T.; Honda, Y.; Kitao, O.; Nakai, H.; Klene, M.; Li, X.; Knox, J. E.; Hratchian, H. P.; Cross, J. B.; Bakken, V.; Adamo, C.; Jaramillo, J.; Gomperts, R.; Stratmann, R. E.; Yazyev, O.; Austin, A. J.; Cammi, R.; Pomelli, C.; Ochterski, J. W.; Ayala, P. Y.; Morokuma, K.; Voth, G. A.; Salvador, P.; Dannenberg, J. J.; Zakrzewski, V. G.; Dapprich, S.; Daniels, A. D.; Strain, M. C.; Farkas, O.; Malick, D. K.; Rabuck, A. D.; Raghavachari, K.; Foresman, J. B.; Ortiz, J. V.; Cui, Q.; Baboul, A. G.; Clifford, S.; Cioslowski, J.; Stefanov, B. B.; Liu, G.; Liashenko, A.; Piskorz, P.; Komaromi, I.; Martin, R. L.; Fox, D. J.; Keith, T.; Al-Laham, M. A.; Peng, C. Y.; Nanayakkara, A.; Challacombe, M.; Gill, P. M. W.; Johnson, B.; Chen, W.; Wong, M. W.; Gonzalez, C.; Pople, J. A. *Gaussian 03* , Revision C.02; Gaussian, Inc., Wallingford, CT, 2004.
(65) Becke, A. D. *J. Chem. Phys.* **1993**, *98*, 5648–5652.
(66) Goto K.; van de Geijn, R. A. *ACM Transactions on Mathematical Software* **2008**, *34*, Article 12.
(67) (a) Nicklass, A.; Dolg, M.; Stoll, H.; Preuss, H. *J. Chem. Phys.* **1995**, *102*, 8942–8952. (b) Cao, X. Y.; Dolg, M. *J. Chem. Phys.* **2001**, *115*, 7348–7355. and references cited therein.
(68) McLean, A. D.; Chandler, G. S. *J. Chem. Phys.* **1980**, *72*, 5639–5648.

and Bernardi.[69] These converged geometries were used to obtain frequencies in the harmonic approximation; the calculations were again corrected for BSSE. It is well-known that B3LYP overestimates the calculated frequencies[70,71] and thus the frequencies were scaled by 0.9775 to compensate. This particular scaling factor was found to yield optimal agreement between the calculated and experimental frequencies.[70] Some initial analysis on these calculations was performed with use of the GaussSum program.[72] Finally, spectra were generated from the IR intensities by broadening each of the IR lines with a Lorentzian of width 12 $cm^{-1}$, using software developed in-house. These spectra were subsequently compared to experiment. Structural assignment of the ions was achieved by comparison of the recorded spectra with calculated spectra derived from the gas phase structures identified by theory.

(69) Boys, S. F.; Bernardi, F. *Mol. Phys.* **1970**, *19*, 553–566.
(70) Irikura, K. K.; Johnson, R. D.; Kacker, R. N. *J. Phys. Chem. A* **2005**, *109*, 8430–8437.
(71) Foresman, J. B.; Frisch, A. E. *Exploring Chemistry with Electronic Structure Methods*, 2nd ed.; Gaussian Inc.: Pittsburgh, PA, 1996.
(72) O'Boyle, N. M.; Tenderholt, A. L.; Langner, K. M. *J. Comput. Chem.* **2008**, *29*, 839–845.

**Acknowledgment.** Financial support by the "Nederlandse Organisatie voor Wetenschappelijk Onderzoek" and the German Research Foundation (DFG) is acknowledged. The authors thank Dr. Britta Redlich for her skillful assistance at the FELIX facility.

**Supporting Information Available:** Additional Figures 1S−7S and Scheme 1S (referred to in the text), videoclip of the computed vibration at 1620 $cm^{-1}$ in **2b-(b)**, calculated coordinates and energies of all reported ion structures, and calculated coordinates and energies of additional structures required to determine DMF binding energies. This material is available free of charge via the Internet at http://pubs.acs.org.